ELSEVIER

Journal of Chromatography A, 786 (1997) 195–207

JOURNAL OF CHROMATOGRAPHY A

Extension of the shock layer theory to the case of a linear dependence of the axial dispersion and the mass transfer coefficients on the concentration

Peter Sajonz[a,b], Guoming Zhong[a,b], Georges Guiochon[a,b,*]

[a]*Department of Chemistry, University of Tennessee, Knoxville, TN 37996-1600, USA*

[b]*Chemical and Analytical Sciences Division, Oak Ridge National Laboratory, Oak Ridge, TN 37831-6120, USA*

Received 14 February 1997; received in revised form 23 May 1997; accepted 23 May 1997

Abstract

The classical shock layer theory assumes that the coefficients of axial dispersion and of mass transfer kinetics are constant. Experimental results have shown that this assumption is not always valid. The influence of a linear dependence of these coefficients on the concentration is investigated. The shock layer theory is easily extended to this case and an analytical solution is reported. Changes in the shape of the breakthrough curves and in the thickness of the shock layer are discussed. Excellent agreement was observed between the results of numerical calculations of breakthrough curves and the shock layer thickness derived from the analytical solution. The agreement found with experimental results previously reported was also excellent. © 1997 Elsevier Science B.V.

Keywords: Axial dispersion; Mass transfer; Shock layer; Non-linear chromatography; Band profiles

1. Introduction

The modeling of the band profiles obtained in non-linear chromatography is best carried out with the simplest model that affords realistic results [1]. In most instances, the efficiency achieved in high-performance liquid chromatography (HPLC) is high. This justifies considering axial dispersion as a correction to the predictions of the ideal model and using the equilibrium-dispersive model [1]. With this model, apparent axial dispersion is due to the combination of the effects of the axial concentration gradients (axial diffusion), of convection in the mobile phase percolating through the column bed (eddy diffusion) and of the finite rate of mass transfers across the column. While the influence of the first two terms remains small in practically all cases encountered in laboratory or industrial applications of HPLC, this is not true of the last one. When the retention mechanism involves the formation of strong chemical bonds (e.g., complexation) or of multi-site interactions (e.g., adsorption or ion-exchange of polymers, such as proteins), the kinetics of adsorption/desorption tends to become slow. Large-size molecules have low diffusivities and their migration across the network of pores of porous particles or the network of cross-linked polymeric chains in resin particles tends to be slow. For these

*Corresponding author. Address for correspondence: Department of Chemistry, University of Tennessee, Knoxville, TN 37996-1600, USA.

PII S0021-9673(97)00591-8

reasons, more sophisticated kinetic models must be used.

The concept of shock layer is germane to lumped kinetic models. If, as is the most common case, the equilibrium isotherm is convex upwards, the high concentrations of a breakthrough curve move faster than the low ones [1]. The profile is self-sharpening. In the absence of axial dispersion, a vertical concentration profile or shock would be recorded. Under non-ideal conditions, a balance between the self-sharpening trend caused by the non-linear thermodynamics on the one hand and the apparent axial dispersion, originating from axial diffusion, eddy dispersion and the finite rate of mass transfers, on the other hand is reached progressively. The most powerful theoretical tool available for the study of the propagation of these self-sharpening fronts in chromatography is the shock layer theory, suggested originally by Rosen [2], used by Glueckauf [3], and developed by Rhee et al. [4], Rhee and Amundson [5] and by Gorius et al. [6]. Although this steady-state profile is asymptotic [4,5], in practice, it is reached after a relatively short migration distance [7,8]. Simple considerations developed by Rhee et al. [4,5] have lead them to define a shock layer thickness (SLT) that characterizes the combined influence of the various sources of non-ideal behavior on the band profile. The SLT is a function of the axial dispersion coefficient and of the rate constant of mass transfer. Thus, the SLT is a very convenient parameter to characterize the apparent column dispersion in non-linear chromatography. In this area, it should play a role similar to the one of the height equivalent to a theoretical plate (HETP) in analytical, i.e., linear chromatography.

In all kinetic models of chromatography, however, the parameters describing the mass transfer kinetics are traditionally assumed to be constant. There is increasing experimental evidence that this not always the case [9–14]. Significant dependence of the coefficients of mass transfer and of the diffusivity on the concentration in the range of concentrations used in preparative chromatography was reported recently by different authors [12–14], using a variety of systems. The concept of SLT has been proven so useful [1] that it is important to discuss the possibility of its extension to cases where the coefficients of axial dispersion and of mass transfer kinetics are concentration-dependent.

In this paper, we present a detailed discussion of the extension of the shock layer theory to the case in which the coefficients of the mass transfer kinetics and the axial dispersion depend on the concentration. The linear dependence suggested by experimental results [14] has been adopted. Following the original approach of Rhee et al. [4,5], an algebraic solution could be derived, as recently suggested [15–19]. Its properties are studied and discussed. This algebraic solution was also compared to numerical solutions of the same model, which include no simplifications.

2. Theoretical

First, we present briefly the transport-dispersive model, a simple non-equilibrium model of chromatography, including convection, axial dispersion and lumped mass transfer kinetics in the stationary phase. Then, we show how the shock layer theory can be extended to cases in which the Peclet and Stanton numbers are both functions of the solute concentration.

2.1. Transport-dispersive model

2.1.1. Differential mass balance equation of chromatography

This equation is written

$$\frac{\partial C}{\partial t} + F\frac{\partial q}{\partial t} + u\frac{\partial C}{\partial z} = \frac{\partial}{\partial z}\left[D_L\frac{\partial C}{\partial z}\right] \quad (1)$$

where C and q are the concentrations of the sample in the mobile and the stationary phase, respectively, z and t are distance and time, respectively, F is the phase ratio ($F=(1-\varepsilon)/\varepsilon$, with ε being the total column porosity), u is the mobile phase velocity and D_L is the axial dispersion coefficient which, in this case, depends linearly on the concentration.

2.1.2. Mass transfer kinetics

We consider a solid film linear driving force model to represent the kinetics [1]

$$\frac{\partial q}{\partial t} = k_f(q^* - q) \quad (2)$$

where k_f is the overall mass transfer rate coefficient, a function of the mobile phase concentration, and q^* is the adsorbed phase concentration of the solute

when the stationary phase is in equilibrium with the mobile phase concentration, C, as given by the isotherm. When $k_f \to \infty$, there is increasingly fast equilibration between the two phases. The limit, $k_f = \infty$, corresponds to the achievement of instantaneous equilibrium between both phases. The ideal model corresponds to both $k_f = \infty$ and $D_L = 0$.

2.1.3. Equilibrium isotherm

The Langmuir isotherm is used to account for the adsorption equilibrium

$$q^* = \frac{aC}{1 + bC} \tag{3}$$

Its numerical coefficients, a and b, are independent of the concentration.

2.1.4. Concentration dependence of D_L and k_f

The results of experimental observations [13,14] suggest that a linear relationship is valid in a rather wide concentration range. Accordingly, we assume in this work a linear dependence of the axial dispersion coefficient and the rate coefficient on the concentration, with

$$D_L = D_L^0 + D_L^1 C \tag{4a}$$

$$k_f = k_f^0 + k_f^1 C \tag{4b}$$

where D_L^0, D_L^1, k_f^0 and k_f^1 are numerical coefficients.

Accordingly, the Peclet and Stanton numbers become related to the concentration through

$$Pe = \frac{uL}{D_L^0 + D_L^1 C} = \frac{uL}{D_L^0}\left(\frac{1}{1 + \frac{D_L^1}{D_L^0}C}\right) = \frac{Pe^0}{1 + Pe^1 C} \tag{4c}$$

$$St = \frac{(k_f^0 + k_f^1 C)L}{u} = \frac{k_f^0 L}{u}\left(1 + \frac{k_f^1}{k_f^0}C\right) = St^0(1 + St^1 C) \tag{4d}$$

with $Pe^0 = uL/D_L^0$, $Pe^1 = D_L^1/D_L^0$, $St^0 = k_f^0 L/u$ and $St^1 = k_f^1/k_f^0$.

2.1.5. Initial and boundary conditions

The initial and boundary conditions of the problem correspond to a column that is initially filled with mobile phase at a concentration, C^r (usually equal to 0), and to the step injection of a solution of the component at a concentration, C^1, respectively. The boundary condition includes the classical Danckwerts condition, as applied classically in chromatography [1].

These conditions are written

$$C(z, 0) = 0$$

$$uC(0, t) - D_L \frac{\partial C}{\partial z}(0, t) = uC^1 \quad \text{for } t \geq 0$$

$$\frac{\partial C}{\partial z}(L, t) = 0 \tag{5}$$

2.1.6. Dimensionless system of equations

The system of Eqs. (1)–(5), (5) states the transport-dispersive or lumped kinetic model for concentration-dependent axial dispersion and mass transfer rate coefficients. It is convenient for the following discussion to recast these equations under dimensionless forms

$$\frac{\partial C}{\partial \tau} + \frac{\partial C}{\partial x} - \frac{\partial}{\partial x}\left(\frac{1}{Pe}\frac{\partial C}{\partial x}\right) + F\frac{\partial q}{\partial \tau} = 0 \tag{6}$$

$$\frac{\partial q}{\partial \tau} = St(q^* - q) \tag{7}$$

with the following dimensionless variables and parameters:

$$\tau = \frac{ut}{L} \tag{8a}$$

$$x = \frac{z}{L} \tag{8b}$$

$$Pe = \frac{uL}{D_L} \tag{8c}$$

$$St = \frac{k_f L}{u} \tag{8d}$$

This system can be solved numerically, using an appropriate calculation method. A finite difference method was used in this work [1,18–20]. Provided that some simplifying assumptions are made, an analytical solution can be derived, using the classical shock layer theory [5].

2.2. Shock layer theory

The same approach followed in the classical shock

layer theory can be applied when the parameters of the system of Eqs. (1)–(3), (4a)–(4d), (5) are concentration-dependent. As in the case of constant coefficients, we look for an asymptotic solution of the system of Eqs. (6) and (7). Assuming that this solution exists [4,5], the concentration profile should move along the column unchanged in shape, as a constant pattern migrating at a constant dimensionless velocity, λ. A coordinate transform allows the use of a moving coordinate system

$$\xi = x - \lambda\tau \tag{9}$$

The constant migration velocity, λ, of the profile in the reduced coordinate system will be shown later to be equal to the reduced velocity of the shock in the ideal model. With this transform, q and C become functions of the coordinate ξ alone. For an asymptotic solution, the boundary conditions are

$$C(\xi = -\infty) = C^{\mathrm{l}},$$
$$\frac{\partial C}{\partial \xi}(\xi = -\infty) = \frac{\partial q}{\partial \xi}(\xi = -\infty) = 0 \tag{10a}$$

$$C(\xi = +\infty) = C^{\mathrm{r}},$$
$$\frac{\partial C}{\partial \xi}(\xi = +\infty) = \frac{\partial q}{\partial \xi}(\xi = +\infty) = 0 \tag{10b}$$

Eqs. (6) and (7) can be combined following the procedure described by Rhee et al. [4,5] and rearranged into the equation

$$-\frac{\lambda}{St(C)}\frac{\partial}{\partial \xi}\left(\frac{1}{Pe}\frac{\partial C}{\partial \xi}\right) + \left(\frac{1}{Pe} + \frac{\lambda(1-\lambda)}{St}\right)\frac{\partial C}{\partial \xi} =$$
$$(1-\lambda)(C - C^{\mathrm{l}}) - F\lambda(q^*(C) - q^*(C^{\mathrm{l}})) =$$
$$G(C, C^{\mathrm{l}}, C^{\mathrm{r}}) \tag{11}$$

Integration of Eq. (11) gives the asymptotic concentration profile. Unfortunately, it is not possible to integrate this equation in the general case. Following Rhee et al. [4,5], we neglect the first term on the left hand side (LHS) of Eq. (11). This simplification is necessary to permit the integration of Eq. (11). It requires that the product $Pe\ St$ be very large. The validity of this assumption under typical conditions of non-linear HPLC has been discussed previously [1]. It was shown that this requirement is satisfied in most practical cases encountered in preparative chromatography. The validity of the assumption is illustrated by the excellent agreement observed between the numerical and the analytical solutions presented later, in Section 3.

Applying the boundary condition of Eq. (10b) to Eq. (11) ($\partial C/\partial \xi = 0$) gives the value of λ

$$\lambda = \left(1 + F\frac{q^{*,\mathrm{l}} - q^{*,\mathrm{r}}}{C^{\mathrm{l}} - C^{\mathrm{r}}}\right)^{-1} \tag{12}$$

Eq. (12) shows that λ is the dimensionless shock layer velocity, which is consistent with the initial assumption (Eq. (9)). The actual migration velocity of the shock layer (e.g., in m/s) is

$$u_{\mathrm{s}} = \lambda u \tag{13}$$

The shock layer velocity does not depend on the axial dispersion coefficient nor on the rate coefficient of the mass transfer kinetics, whether these coefficients are constant (as assumed by Rosen [2], Glueckauf [3], Rhee et al. [4] and Rhee and Amundson [5]) or concentration-dependent (as assumed here). It is a function of the concentration solely through the isotherm (Eqs. (3) and (12)) and it is the same as the velocity of the shock in the ideal model.

Since we are interested in the concentration profile of the breakthrough curve in the region where the concentration varies significantly, we define this region of interest through two intermediate concentrations, C^{ls} and C^{rs}, corresponding respectively to the initial and the final concentrations of the profile in the range considered. These concentrations are defined as follows

$$C^{\mathrm{ls}} = C^{\mathrm{l}} + \theta(C^{\mathrm{r}} - C^{\mathrm{l}}) \tag{14a}$$

$$C^{\mathrm{rs}} = C^{\mathrm{r}} - \theta(C^{\mathrm{r}} - C^{\mathrm{l}}) \tag{14b}$$

where θ is smaller than 0.5. In numerical and experimental applications, θ is usually taken as being equal to 0.05. The SLT is defined as the distance between these two concentrations in the asymptotic profile. From Eq. (11), simplified as discussed above, the SLT is given by the following equation

$$\Delta\xi = \int_{C^{\mathrm{ls}}}^{C^{\mathrm{rs}}} \left[\frac{1}{Pe(C)} + \frac{\lambda(1-\lambda)}{St(C)}\right] G^{-1}(C, C^{\mathrm{l}}, C^{\mathrm{r}})\, dC \tag{15}$$

where $G^{-1}(C, C^{\mathrm{l}}, C^{\mathrm{r}})$ is a function of the isotherm

and of the initial (C^{I}) and final (C^{r}) concentrations of the breakthrough profile [4,5]. This equation is simple to integrate in the case of a Langmuir isotherm, whether in the case of constant coefficients [6–8] or in the case of coefficients that depend linearly on the concentration (Eqs. (4a)–(4d)). Using conventional algebraic manipulations, the following equation giving the thickness of the shock layer is derived from Eq. (15)

$$\Delta\xi = \frac{1+\dfrac{1}{k_0' R^{I}}}{1-R^{I}} \left\{ \frac{1}{Pe^{0}} \left[(1+R^{I}+Pe^{I}C^{I}) \ln\left(\frac{1-\theta}{\theta}\right) + Pe^{I}C^{I}(1-2\theta)(1-R^{I}) \right] + \frac{\lambda(1-\lambda)}{St^{0}} \left[\left(R^{I}+\frac{1}{1+St^{I}C^{I}}\right) \ln\left(\frac{1-\theta}{\theta}\right) + \left(R^{I}-\frac{1}{1+St^{I}C^{I}}\right) \times \ln\left(\frac{1+St^{I}C^{I}\theta}{1+St^{I}C^{I}(1-\theta)}\right) \right] \right\} \quad (16)$$

where $R^{I}=1/(1+bC^{I})$.

The concentration profile of the component in the shock layer as discussed above is a concentration profile along the ξ axis. Its thickness, given by Eq. (16), is measured along this axis. It is easy to derive from this expression the thickness of the breakthrough curves expressed in different units, e.g., column length, time, or reduced-time units. Depending on the nature of the experiments performed, one expression may be more convenient for practical purposes. In the following discussion, we use reduced-time units and the SLT is given by

$$\Delta\tau = \frac{1}{\lambda}\Delta\xi \quad (17)$$

When the axial dispersion coefficient and the rate of the mass transfer kinetics are both independent of the concentration, $Pe^{I}=St^{I}=0$ and Eq. (16) reduces to

$$\Delta\xi = \frac{1+R^{I}}{1-R^{I}} \left(1+\frac{1}{k_0' R^{I}}\right) \left[\frac{1}{Pe^{0}} + \frac{\lambda(1-\lambda)}{St^{0}} \right] \times \ln\left(\frac{1-\theta}{\theta}\right) \quad (18)$$

which is exactly the same equation as the one derived directly in the case of constant Peclet and Stanton numbers [1,4,5,7,8].

3. Illustrations and discussion

Calculated breakthrough curves were obtained corresponding to a variety of experimental conditions illustrating the influence on the shock layer profiles of the concentration dependence of the axial dispersion coefficient and the rate of the mass transfer kinetics for a wide range of values of the different coefficients. The SLTs were calculated either from the numerical solutions of the system of Eqs. (1)–(3), (4a)–(4d), or from the algebraic solution (Eq. (16)) of the asymptotic Eq. (11). The results are compared in order to validate the analytical, asymptotic solution.

The values of the parameters used in the calculations are: $F=0.449$; $C^{r}=0$, $C^{I}=25$ mg/ml (kg/m^3); $a=12$ and $b=0.024$ ml/mg (m^3/kg). The breakthrough curves are plotted as concentration versus the reduced time, defined as $\tau=t/t_0$, where $t_0=L/u$ is the hold-up time of the column.

3.1. Velocity of the shock layer

Eq. (12) shows that the velocity of the shock layer is constant. As long as the axial concentration profile is a constant pattern, all of its points move along the column at the same velocity. However, because of the finite thickness of the shock layer, only one point of the concentration profile elutes at the same time as the shock of the ideal model, i.e., with a retention time equal to $1/\lambda=1+F\Delta q/\Delta C$, corresponding to the equilibrium isotherm. This point is usually not identical to the half-height of the breakthrough curve. Its relative height depends on the value of the two coefficients D_L and k_f, hence it is affected by their concentration dependence. This implies that deriving isotherm data from the retention time or volume of a particular point of the breakthrough curve is erroneous, as has been observed experimentally long ago [21]. The only correct procedure to define and measure the retention time of

the breakthrough curve is through an integral mass balance, using the moment or area method, which affords the exact retention time [15,16] and gives accurate isotherm data.

In the numerical results presented here, the reduced velocity of the shock layer, λ, is 0.23. The dimensionless retention time of the breakthrough curve is $t_R/t_0 = L/(u_s t_0) = 1/\lambda = 4.37$. The breakthrough curves shown in all figures have that same retention time.

3.2. Breakthrough curves and shock layer thickness

One of the important features of Eq. (11) is that, once the first term on the LHS is neglected, the roles played by the Peclet and the Stanton numbers are symmetrical. The same result is of course observed in Eq. (16). The contributions to the SLT due to mass transfer kinetics (St) and to axial dispersion (Pe) are additive. Accordingly, these two parameters can be conveniently discussed separately and successively, which simplifies the study of their influence and clarifies the presentation of the results. The total effect of these two phenomena can be obtained by the addition of their respective contributions.

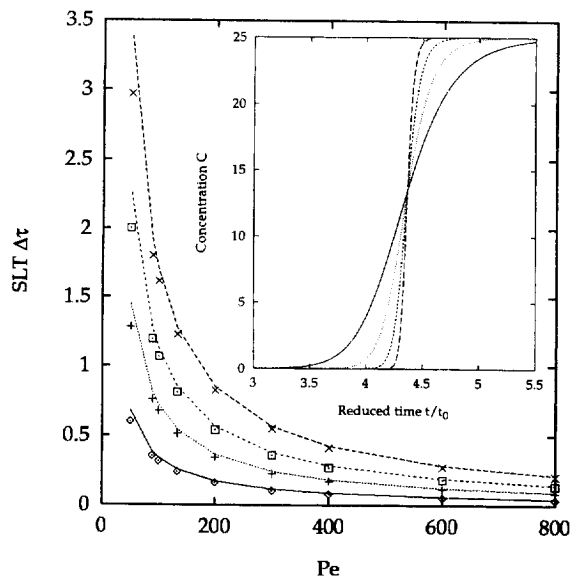

Fig. 1. Comparison of the shock layer thickness derived from the analytical solution and from numerical calculations. The lines represent the analytical solution for different values of θ. The symbols represent the results of numerical calculations. The following values of θ were used for measuring the shock layer thickness: long-dashed line and ×, 0.001; short-dashed line and □, 0.01; dotted line and +, 0.05; solid line and ◇, 0.2. Inset: breakthrough curves from numerical calculations. Solid line, Pe = 50; dotted line, 100; short-dashed line, 200; long-dashed line, 400.

3.2.1. Shock layer thickness caused by axial dispersion ($St = \infty$)

We present briefly the results obtained with constant coefficients. Then we study the influence of the concentration dependence of the Peclet number by comparing profiles obtained with different relationships between the axial dispersion coefficient and the concentration (i.e., different coefficients in Eqs. (4a) and (4c)) but with the same initial or final value of the Peclet number.

3.2.1.1. Constant Peclet number

The SLT for breakthrough curves with different constant values of Pe is shown in Fig. 1 for θ from 0.1 to 20%. The corresponding breakthrough curves are shown in the inset. The SLT increases with decreasing Peclet number and with decreasing value of θ. As expected, there is an excellent agreement between the values of the SLT derived from the analytical solution in Eq. (16) (lines) and from the profiles obtained by numerical calculation (symbols).

3.2.1.2. Same initial or final value of Pe

Fig. 2a shows breakthrough curves calculated with the same initial value of Pe ($Pe^0 = 500$), but with different values of Pe^1, all of which were negative. In this case, Pe decreases with increasing concentration and the breakthrough curves become quite unsymmetrical, while they are nearly symmetrical in the case in which Pe is constant and equal to 500 (solid line). The upper part of the breakthrough curve is more diffuse than the lower part. The difference between the upper and lower parts of the curve increases with increasing absolute value of Pe^1. The converse case ($Pe^1 > 0$) is illustrated in Fig. 2b. Then, Pe increases with increasing concentration and reaches the same final value, Pe =

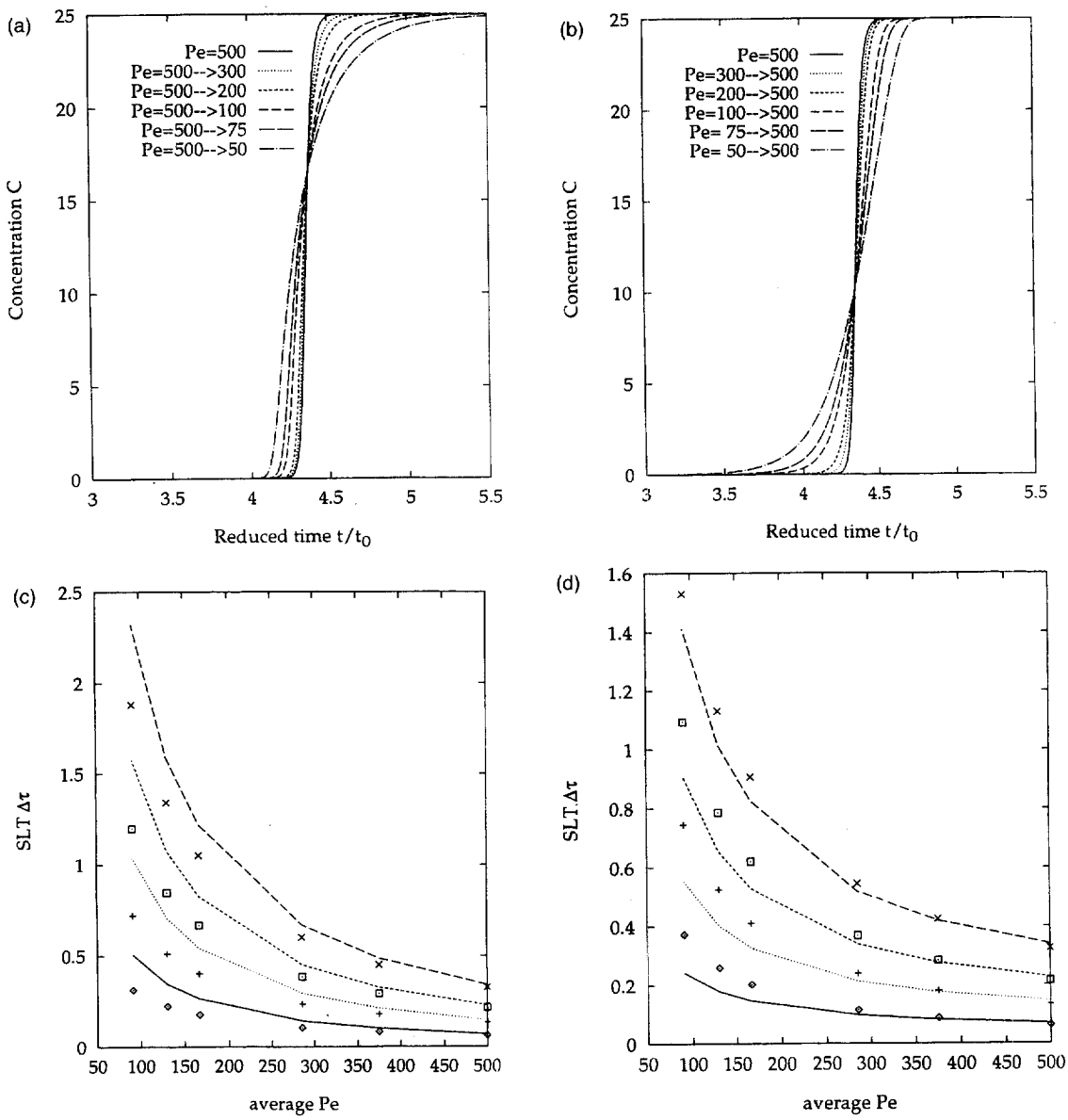

Fig. 2. Shock layer thickness caused by axial dispersion. Same initial or final values of $Pe(C)$. (a) and (b), Breakthrough curves obtained from numerical calculations. The constant initial (a) or final (b) value of Pe is 500. Solid line, constant $Pe = 500$; dotted line, 500→300 or 300→500; short-dashed line, 500→200 or 200→500; middle-dashed line, 500→100 or 100→500; long-dashed line, 500→75 or 75→500; dash-dotted line, 500→50 or 50→500. (c) and (d), Comparison of the values of the shock layer thickness derived from the analytical solution (lines) and from the breakthrough curves resulting from numerical calculations and shown in Fig. 2a (c) and Fig. 2b (d). The average value of Pe varies from 91 to 500. Lines and symbols as in Fig. 1.

500. The breakthrough curves are also unsymmetrical and increasingly so when Pe^{-1} increases. The lower part of the curve is the more diffuse.

In both cases, the SLT decreases with increasing average value of Pe, as shown in Fig. 2c,d. However, for the same average value of Pe, the SLT of the

breakthrough curves obtained is nearly twice as large when *Pe* decreases during the elution of the breakthrough curve (Fig. 2c) than when it increases during this elution (Fig. 2d). In the former case, the values of the SLT obtained from numerical solutions (symbols) are slightly smaller than those predicted by Eq. (17) (lines, Fig. 2c), while the converse is true in the latter case (Fig. 2d). The effect is noticeable only at low average values of the Peclet number.

3.2.2. Shock layer thickness caused by mass transfer kinetics ($Pe = \infty$)

We consider now the influence on the SLT of the concentration dependence of the sole rate coefficient of the mass transfer kinetics, as characterized by the Stanton number, $St = k_f L/u$. The results obtained are quite similar to those calculated in the study of the influence of the concentration on the dispersion coefficient alone. We present briefly the results obtained with constant coefficients and then discuss the influence of the concentration dependence by considering cases in which the initial or final value of the Stanton number are the same.

3.2.2.1. Constant Stanton number

As in the study of the Peclet number, larger values of *St* or θ give sharper breakthrough profiles, hence smaller SLTs, as illustrated in Fig. 3. The corresponding breakthrough curves are shown in the inset. Note that in preparative chromatography, u is usually of the order of 0.1 cm/s, L is of the order of 30 cm and, unless k_f is abnormally small, *St* will most often exceed one or several hundreds.

3.2.2.2. Same initial or final value of the Stanton number

Breakthrough curves calculated with linearly decreasing values of the Stanton number, starting from the same initial value ($St = 50$) are shown in Fig. 4a. Similar curves, calculated with linearly increasing values of *St* ending with the same value, $St = 50$, are shown in Fig. 4b. The corresponding values of the SLT are plotted versus the average value of *St* in Fig. 4c–d, respectively. As was observed in the study of the influence of the Peclet number, the curves become increasingly unsymmetrical when the change in value of *St* during the experiment becomes important. The upper part of the breakthrough curve

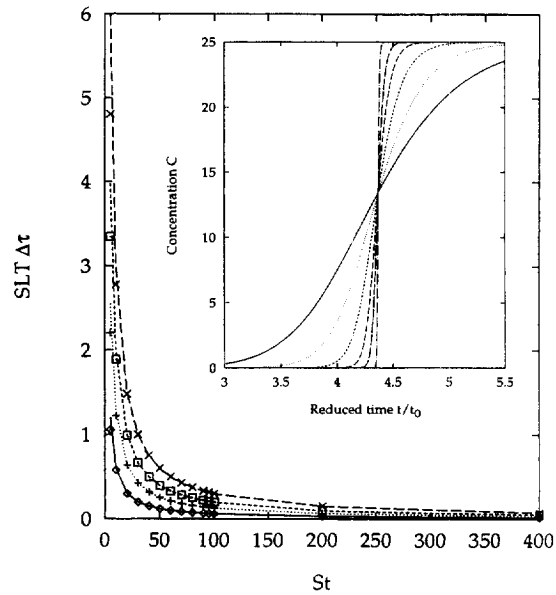

Fig. 3. Comparison of the shock layer thickness derived from the analytical solution (lines) and from numerical calculations (symbols). *St* ranges between 5 and 400. The lines represent the analytical solution for different values of θ. The symbols represent the results of numerical calculations. Symbols and lines as in Fig. 1. Inset: Breakthrough curves obtained from numerical calculation. $St = 5$, solid line; 10, dotted line; 20, short-dashed line; 40, middle-dashed line; 80, long-dashed line; 400, dash-dotted line.

is more diffuse than the lower one when the Stanton number decreases during the experiment, at a constant average value of *St* (Fig. 4a), while the converse is true when the Stanton number increases during elution (Fig. 4b). The shock layers are thicker in the former case (Fig. 4c) than in the latter (Fig. 4d), especially at large values of θ. In both cases, there is an excellent agreement between the values of the SLT derived from the numerical solutions of the equation system (symbols) and those predicted by Eq. (16) (lines).

3.2.3. Comparison of the effects caused by axial dispersion ($St = \infty$) and by mass transfer kinetics ($Pe = \infty$)

A comparison of Figs. 1 and 2c,d shows that, at a constant average value of the Peclet number, the SLT is smaller when *Pe* increases during the experiment (Fig. 2d) than when it decreases (Fig. 2c). The values of the SLT corresponding to a constant Peclet

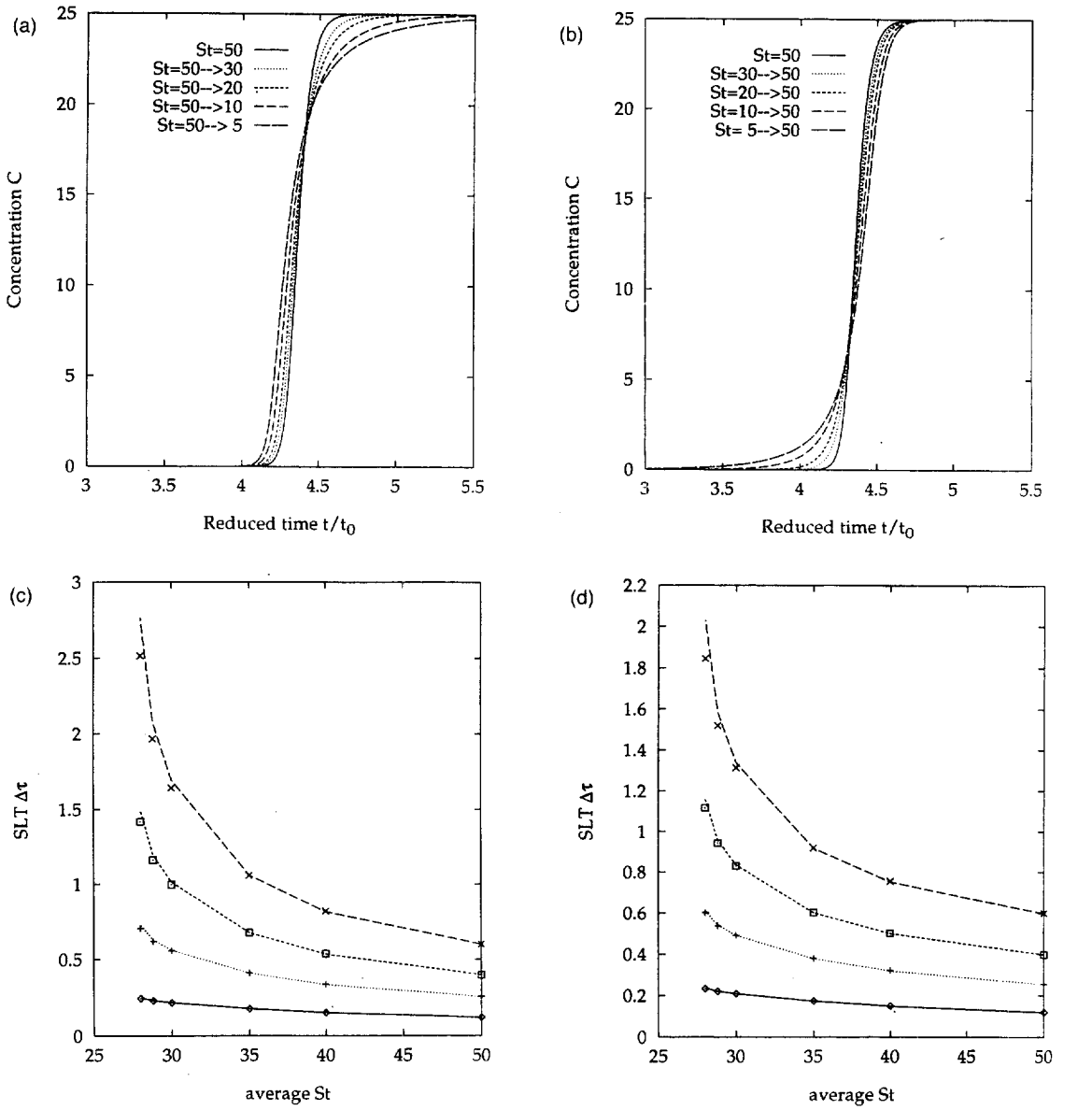

Fig. 4. Shock layer thickness caused by mass transfer kinetics. Same initial or final value of *St*. (a) and (b), Breakthrough curves obtained from numerical calculations. The initial (a) or final (b) value of *St* is 50. Solid line, constant $St=50$; dotted line, 50→30 or 30→50; short-dashed line, 50→20 or 20→50; middle-dashed line, 50→10 or 10→50; long-dashed line, 50→5 or 5→50. (c) and (d). Comparison of the values of the shock layer thickness derived from the analytical solution (lines) and from numerical calculations (symbols) for the profiles in Fig. 4a (c) and Fig. 4b (d). Average value of *St* was between 27.5 and 50. Lines and symbols as in Fig. 1.

number (Fig. 1) are intermediate. These conclusions are confirmed by examination of Eq. (16). The average Peclet number is calculated as $2\{[Pe(0)]^{-1}+[Pe(C^{1})]^{-1}\}^{-1}$, which represents an arithmetic averaging of the influence of the concentration-dependent axial dispersion coefficient, D_L, over the entire concentration step (Eq. (4a)).

A comparison of Figs. 3 and 4c,d shows that, at a

constant average value of the Stanton number, the SLT is smaller when St increases during the experiment (Fig. 3d) than when it decreases (Fig. 3c). However, the SLT obtained at a constant St number is still smaller than the value obtained for an increasing Stanton number (with the same average number). Examination of Eq. (16) confirms that the SLT (for the same average value of St) is always larger if $St_1 \neq 0$ than if $St_1 = 0$. The average of the Stanton number is given by $[St(0)+St(C^1)]/2$, which represents an arithmetic average of the rate constant, k_f, for the highest and lowest concentrations in the step injection (Eq. (4b)), in agreement with experimental results [14]. Even though a definition of an average value is somewhat arbitrary, it is useful to compare different breakthrough curves obtained with different concentration dependencies of the coefficients. This issue is discussed in more detail in the following.

Fig. 5 shows the SLT calculated from Eq. (16), for three different values of the parameter $b = 0.024$, 0.048 and 0.096 ml/mg as a function of $\Delta Pe = Pe(C^1) - Pe(0)$. The value ΔPe determines the extent or strength of the concentration dependence. It is negative when the Peclet number decreases with increasing concentration, positive when the Peclet number increases with increasing concentration, and zero for a constant Peclet number. All values of the SLT are reported to the average value of the Peclet number (as defined earlier, here $Pe_{av} = 88.9$). We can see that when the Peclet number decreases with increasing concentration ($\Delta Pe < 0$), the band is broader than when it increases. The SLT is larger in the former case (i.e. $Pe^1 < 0$) than in the latter (i.e. $Pe^1 > 0$). In the case in which the Peclet number remains constant ($Pe^1 = 0$), the value of the SLT is intermediate. This is true for all values of b. The b-value is seen to have merely a sharpening influence on the breakthrough curve; the SLT is smaller for larger b-values, the general conclusions derived above remaining unchanged[1]. The same is true in the case of an increasing value of C^1, which has an effect similar to that of an increase of b (not shown), i.e., it enhances the non-linear effects. In the constant case ($Pe^1 = 0$), one would obtain the same result for the SLT by either modifying C^1 or b because the product $b\ C^1$ is the important parameter characterizing the intensity of non-linear behavior. However, in the concentration-dependent case, the parameter C^1 also influences the SLT through the concentration dependence of the coefficients (see Eqs. (4a)–(4d)).

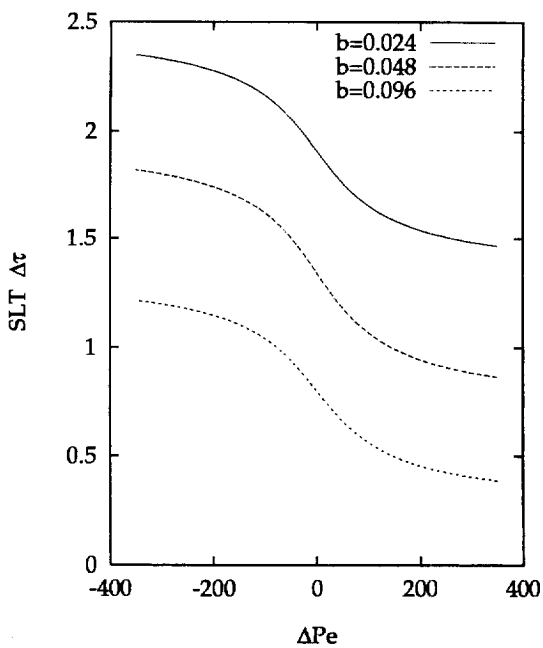

Fig. 5. Dependence of the SLT on the extent of the concentration dependence of Pe. The average value of Pe has been kept constant. $Pe_{av} = 88.9$, $a = 12$, $C^1 = 25$. SLT calculated for different values of $b = 0.024$, 0.048, 0.096 ml/mg, $\theta = 0.001$.

Fig. 6 illustrates the dependence of the SLT, calculated from Eq. (16) for different values of b and the same average value of the Stanton number $St_{av} = 50$, on $\Delta St = St(C^1) - St(0)$. The results observed are different from those found with the Peclet number. When the Stanton number decreases with increasing concentration, the SLT increases with increasing concentration, which is unfavorable, but the same is also true when the Stanton number increases with increasing concentration ($St^1 > 0$). However, the

[1] The problem becomes irrelevant for extremely large values of b. When $b \to \infty$, either $q = a/b$ is constant, in which case $t_R(C = 0) \to \infty$ and the isotherm becomes rectangular, or a remains finite, in which case $q \to 0$ and the retention disappears.

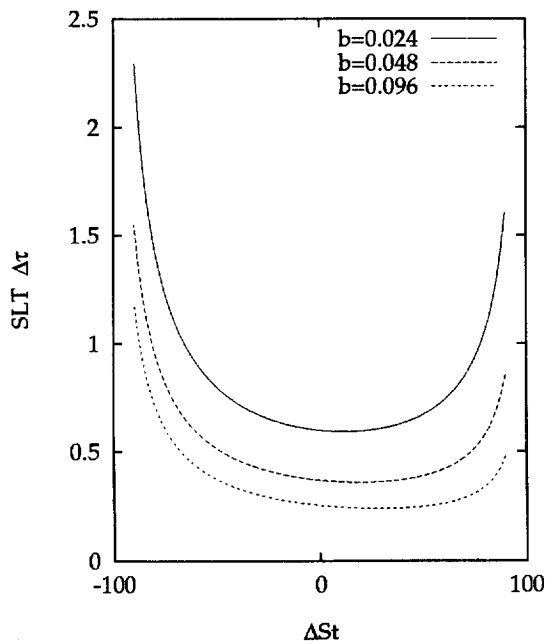

Fig. 6. Dependence of the SLT on the extent of the concentration dependence of St. The average value of St has been kept constant. $St_{av}=50$, $a=12$, $C^{I}=25$. SLT for different values of $b=0.024$, 0.048, 0.096 ml/mg, $\theta=0.001$.

curves tend to be very flat around the center, meaning that slowly increasing St numbers cause only moderate changes of the SLT (see the minima of the curves in Fig. 6). A large b-value causes a decrease in the SLT. However, the location of the minimum value of the SLT tends to drift towards higher values of ΔSt when b increases. The effect of a change in C^{I} is similar to that of changing b (not shown) because, as already mentioned, the product b C^{I} is the important parameter, characterizing the intensity of the non-linear effects.

These results show that the two classical, simple models of chromatography, the equilibrium-dispersive model ($k_f \rightarrow \infty$) and the transport model ($Pe \rightarrow \infty$) give different conclusions regarding the band broadening effects if their coefficients depend on the concentration. In other words, the two models are not equivalent and will not give the same band profiles, even if the coefficients have been properly identified and adjusted to give the same results under linear conditions. This conclusion is the same as was previously derived [22,23] but it is achieved following an entirely different approach. It can be further substantiated by a comparison of the terms in Eq. (16) including Pe^{I} (first line) with those including St^{I} (second line). They are certainly quite different.

Finally, it is worth noting that it is possible to derive from Eq. (11) not only the SLT (Eq. (16)) but also the relationship between the local concentration, C, and the reduced coordinate, ξ, i.e., the equation of the whole concentration profile of the shock layer (in reduced or dimensionless coordinates). However, this equation is complex to use in the case of concentration-dependent axial dispersion and mass transfer rate coefficients. It will not be discussed further here.

4. Conclusion

The classical shock layer concept was easily extended to the case in which the coefficients of axial dispersion and the mass transfer kinetics depend linearly on the sample concentration. A more complex (i.e., a non-linear) concentration dependence could be handled following the same procedure. Depending on the problem studied, numerical solutions of the band profiles or the algebraic equations giving the band profile and the SLT can be used. A comparison of the results derived from the algebraic equation giving the SLT and of those derived from numerical solutions of the lumped kinetic model gave excellent agreement. Thus, tools are available for a systematic study of the concentration dependence of the coefficients of models of chromatography from breakthrough curves.

These breakthrough curves become increasingly unsymmetrical when the coefficients of axial dispersion and the mass transfer kinetics depend more strongly on the sample concentration and the changes in value experienced by these coefficients during an experiment increase. The asymmetry has an important effect on the thickness of the shock layer. The symmetry of the roles played under linear conditions by the two causes of band broadening, axial dispersion and mass transfer resistances, is not maintained under non-linear conditions.

5. Symbols

a, b	first and second parameters of the Langmuir isotherm, l, m^3/kg
C	liquid-phase concentration of the component, kg/m^3
C^l, C^r	left and right boundary concentrations, kg/m^3
C^{ls}, C^{rs}	start and end concentrations of the shock layer, kg/m^3
D_L	axial dispersion coefficient, m^2/s
D_L^0, D_L^1	constant and concentration-dependent parts of the dispersion coefficient, m^2/s, $m^5/(s\ kg)$
F	phase ratio
G	function defined by Eq. (11)
k_f	mass transfer coefficient, 1/s
k_f^0, k_f^1	constant and concentration-dependent parts of the rate coefficient, 1/s, $m^3/(s\ kg)$
$k_0' = Fa$	retention factor at infinite dilution
L	column length, m
$Pe = uL/D_L$	Peclet number
Pe_{av}	average Peclet number
Pe^0, Pe^1	constant and concentration-dependent parts of the Peclet number, l, m^3/kg
q	solid-phase concentration, kg/m^3
q^*	solid-phase concentration at equilibrium, kg/m^2
R	$=1/(1+bC)$
St	$=k_f L/u$, Stanton number
St_{av}	average Stanton number
St^0, St^1	constant and concentration-dependent parts of the Stanton number, m^3/kg
t	=time, s
u	liquid-phase flow velocity, m/s
u_ζ	shock layer propagation velocity, m/s
x	$=z/L$ dimensionless axial position in the column
z	axial position in the column, m

Greeks

ε	total column porosity
λ	reduced propagation velocity of the shock layer
τ	$=ut/L$ dimensionless time
θ	Parameter defining the shock layer thickness (Eqs. (14a) and (14b))
ξ	coordinate transform parameter in Eq. (9)
$\Delta\xi$	SLT in the reduced coordinates system
τ	SLT in reduced time units (t/t_0)

Acknowledgements

This work has been supported in part by Grant CHE-9701680 of the National Science Foundation and by the cooperative agreement between the University of Tennessee and the Oak Ridge National Laboratory. We acknowledge the support of Maureen S. Smith in solving our computational problems.

References

[1] G. Guiochon, S.G. Shirazi and A.M. Katti, Fundamentals of Preparative and Nonlinear Chromatography, Academic Press, New York, 1994.
[2] J.B. Rosen, Ph.D. Thesis, Columbia University, New York, 1952.
[3] E. Glueckauf, Trans. Faraday Soc. 51 (1955) 1540.
[4] H.-K. Rhee, B.F. Bodin, N.R. Amundson, Chem. Eng. Sci. 26 (1971) 1571.
[5] H.-K. Rhee and, N.R. Amundson, Chem. Eng. Sci. 27 (1972) 199.
[6] A. Gorius, M. Bailly, D. Tondeur, Chem. Eng. Sci. 46 (1991) 677.
[7] J. Zhu, G. Guiochon, J. Chromatogr. 636 (1993) 189.
[8] J. Zhu, Z. Ma, G. Guiochon, Biotechnol. Prog. 9 (1993) 421.
[9] W. Gallagher, C. Woodward, Biopolymers 28 (1989) 2001.
[10] K. Lederer, J. Amtmann, S. Vijayakumar, J. Billiani, J. Liq. Chromatogr. 13 (1990) 1849.
[11] S. Gibbs, A. Chu, E. Lightfoot, T. Root, J. Phys. Chem. 93 (1991) 467.
[12] B. Al-Duri, G. McKay, J. Chem. Biotechnol. 55 (1992) 245.
[13] A. Seidel-Morgenstern, S.C. Jacobson, G. Guiochon, J. Chromatogr. 637 (1993) 19.
[14] H. Guan-Sajonz, P. Sajonz, G. Zhong, G. Guiochon, Biotechnol. Prog. 12 (1996) 380.
[15] G. Zhong, P. Sajonz, G. Guiochon, Ind. Eng. Chem. Res. 36 (1997) 506.
[16] P. Sajonz, H. Guan-Sajonz, G. Zhong and G. Guiochon, Biotechnol. Prog., in press.
[17] P. Sajonz, G. Zhong, G. Guiochon, J. Chromatogr. A 728 (1996) 15.

[18] C. Hirsch, Numerical Computation of Internal and External Flow, Vol. 2, Wiley, Chichester, 1988.
[19] M. Czok, G. Guiochon, Anal. Chem. 62 (1990) 189.
[20] P. Sajonz, G. Zhong, G. Guiochon, J. Chromatogr. A 731 (1996) 1.
[21] G. Zhong, G. Guiochon, J. Chromatogr. A 721 (1996) 187.
[22] J.F.K. Huber, R.G. Gerritse, J. Chromatogr. 58 (1971) 137.
[23] S. Golshan-Shirazi, G. Guiochon, J. Chromatogr. 603 (1992) 1.